

MEASUREMENT OF QUARTZ CRYSTAL UNITS UP TO 500 MHz
AND ABOVE BY THE USE OF A PI NETWORK WITH ERROR CORRECTION

Bernd W. Neubig

TELE QUARZ GMBH, D-6924 Neckarbischofsheim 2, Fed. Rep. of Germany

At eleva
100 MHz,
phase im
series r
branch (
longer e
in norma
nes). Th
pedance
red to R
(Fig. 4)
until no
cribing

Crystals
than 5 .
is less
sect the
This is
thods ar
MHz.

1.3 New

The new
calibrat
stor. Me
libratio
ideal Pi
Instead
ce of ex
electric
arbitrar
source a
one side
other si
and stra
tance Cc
ween the
calibrat
pendent
figure 5

From fig
ly deriv

a) Pi-ne

b) Pi-ne

c) Pi-ne

R_G : comp
cry:

R_L : comp
cry:

INTRODUCTION

The Pi-Network method according to IEC-publication 444 (DIN 45105) has been widely acknowledged as the measurement standard for quartz crystal units up to 125 MHz. Above this frequency limit, this measurement method leads to insufficient precision or is no longer possible, resp., due to the stronger influence of the static capacitance C_0 .

A new measurement method, the idea of which was first published by F. Neuscheler (1), uses the conventional arrangement with the classical Pi-network applying an error correction method based on an extended calibration procedure. It can also be used with other jigs such as the coaxial jig proposed in EIA 512. During an International Workshop on Crystal Measurement this method was successfully proved to give comparable accuracy and reproducibility up to 1 GHz of EIA 512 as the S-parameter method.

The following paper describes the measurement principle as well as a consideration of errors and presents some results of comparative measurements.

1. IMPEDANCE MEASUREMENT WITH THE PI NETWORK

The determination of the crystal parameters is based on the measurement of the complex impedance by a transmission method. Therefore, the crystal is inserted in a double Pi-network described in IEC-publication 444 (figure 1). This jig consists of two resistive Pi-networks with 50 ohms impedance at the external terminal sides and 12,5 ohms each - i. e. totally 25 ohms - at the crystal terminal sides. The crystal under test (XUT) is forced to have a well-defined position with the contacting points 2 mm off the bottom plate, therefore maintaining the same measurement plane for repeated measurements. The jig is commercially available by TELE QUARZ GMBH and other suppliers.

Figure 2 shows the arrangement of the measurement jig in conjunction with a network analyzer or - alternatively - a combination of frequency generator and vector voltmeter (vector analyzer). The signal is split into two paths by a power divider, thus the voltage at both inputs have approximately the same voltage level.

1.1 Classical method (IEC 444)

In the classical measurement method, the unknown impedance is determined from the complex voltage ratio at the B-channel-output between the short circuited Pi-network and the inserted crystal.

The impedance can be calculated under the assumption that all components of the Pi-network are known and close to ideal. The reflexions caused by impedance mismatch, the spread capacitances and the lead inductances as well as other errors are neglected at this measurement technique.

Equ. 1 shows the formula for the computation of the unknown impedance:

$$R_x = 25 \left\{ \frac{U_{Bk}}{U_b} - 1 \right\} \quad (1)$$

where U_{Bk} is the measured B-channel-voltage with short circuit and U_b is the measured voltage with the unknown impedance R_x . This equation is only valid for an ideal Pi-network with an impedance of exactly 25 ohms "seen" by the crystal. The resonance frequency f_r and resonance resistance R_r are computed from the amplitude at zero phase. The parameters C_1 , L_1 are derived from a Q-measurement by a phase offset-method. C_0 is determined by a separate measurement in a capacitance bridge.

The circuit diagram of the quartz crystal unit assumed in this technique is the well-known van-Dyke model with 4 elements (R_1 , C_1 , L_1 , C_0) according to fig. 3 a.

1.2 Crystals at elevated frequencies

At higher frequencies and wider frequency ranges it is however more convenient to use a more detailed circuit model to represent the electrical characteristics of the crystal. Fig. 3 b shows such a model. In the vicinity of a single resonance this can always be reduced to the simple circuit of Fig. 3 a. A medium complex network according to Fig. 3 c, which considers the effect of the metal enclosure by the two capacitances C_{01} and C_{02} and the losses of the internal mounting structure (springs, cement spots) by an additional parallel conductance G_0 was generally agreed at the recent IEC-TC 49-meeting to be a reasonable model to be applied at higher frequencies.

At elevated frequencies, i. e. above approximately 100 MHz, the resonance frequency f_r with a zero phase impedance moves more and more away from the series resonance frequency f_s of the motional branch (L_1, C_1, R_1) of the crystal. It does no longer exist above approximately 130 ... 150 MHz in normal AT-cut crystals (5th and higher overtones). This is due to the influence of C_0 , the impedance of which can no longer be neglected compared to R_1 . This means that the admittance circle (Fig. 4) moves up with respect to the real axis until no intersection occurs. The parameter describing this is the so-called figure of merit

$$M = \frac{1}{\omega C_0 R_1} \quad (2)$$

Crystals below 100 MHz usually have M 's greater than 5 ... 10. Above 100 MHz, M decreases and if M is less than 2, the circle does no longer intersect the real axis.

This is the reason why zero phase measurement methods are not applicable above approximately 125 MHz.

1.3 New method with error correction

The new measurement technique uses an additional calibration with an open and a calibration resistor. Measuring the voltage with the inserted calibration resistor, the errors caused by the non-ideal Pi-network can be corrected. In other words: Instead of the assumption of a Pi-network impedance of exactly 25 ohms, the new method implies an electrical diagram of the Pi-network or another arbitrary jig, consisting of a transformed voltage source and a complex generator impedance R_G at the one side and a complex load impedance R_L at the other side, which include the stray inductances and stray capacitances etc. A cross-talk capacitance C_{cc} is assumed to model the feedthrough between the pins. It can be derived from the "open" calibration. The elements of this model are independent of the inserted (crystal-) impedance (see figure 5).

From figure 5, the following formulas can be easily derived (excluding C_{cc}):

a) Pi-network with short circuits:

$$\frac{U_n}{U_k} = \frac{R_c + R_L}{R_L} \quad (3)$$

b) Pi-network with calibration resistor R_n

$$\frac{U_n}{U_{rn}} = \frac{R_c + R_L + R_n}{R_L} \quad (4)$$

c) Pi-network with unknown impedance R_x

$$\frac{U_n}{U_{rx}} = \frac{R_c + R_L + R_x}{R_L} \quad (5)$$

R_G : complex source impedance seen from the crystal terminal to the generator

R_L : complex load resistance seen from the crystal terminal to the network analyzer.

R_L and R_G may be different and include all stray capacitances and inductances.

R_n : the calibration resistor, to which the cross-talk capacitance of the Pi-network is in parallel

$$\underline{R}_n = R_n // -j 1 / (\omega C_{cc}) \quad (6)$$

U_G : source voltage of the equivalent electrical diagram

U_{RX} : output voltage with complex load R_L

U_{RN} : output voltage with known calibration impedance R_n

U_K : output voltage with short circuit

With these three measurements, the unknown impedance R_x can be determined taking into account all non-ideal characteristics of the jig. The accuracy of the measurement depends on the precision of the used calibration resistor and the accuracy of the measured voltage and phase only. In the above-mentioned formulas (3), (4) and (5), the voltages U_{RN} , U_K and U_{RX} can also be replaced by the complex voltage ratio of these voltages referred to the reference channel.

From the equations (3), (4) and (5), the unknown impedance including C_{cc}

can be derived as:

$$\underline{R}_x = R_n \frac{(\underline{U}_k / \underline{U}_{rx} - 1)}{(\underline{U}_k / \underline{U}_{rn} - 1)} = \text{Re}(R_x) + j \text{Im}(R_x) \quad (7)$$

The measured voltages or voltage ratios, resp., are complex values which have to be divided into magnitude and phase:

$$\underline{U}_k / \underline{U}_{rx} = U_k / U_{rx} \{ \cos(p_k - p_{rx}) + j \sin(p_k - p_{rx}) \} = x_1 + j y_1 \quad (8)$$

$$\underline{U}_k / \underline{U}_{rn} = U_k / U_{rn} \{ \cos(p_k - p_{rn}) + j \sin(p_k - p_{rn}) \} = x_2 + j y_2 \quad (9)$$

U_k, U_{RX}, U_{RN} - magnitude of the measured voltages

p_k, p_{RX}, p_{RN} - phase values of the measured voltages

The known has equ

Dividing the complex calibration resistance R_N into its real and imaginary part

$$R_N = \text{Re}(R_N) + j \text{Im}(R_N) \quad (10)$$

leads to the real and imaginary part of the unknown impedance (including Ccc):

$$\text{Re}(R_X) = \text{Re}(R_N) x_3 - \text{Im}(R_N) y_3$$

$$\text{Im}(R_X) = \text{Im}(R_N) x_3 + \text{Re}(R_N) y_3$$

$$x_3 = \frac{x_1 (x_2 - 1) + y_1 y_2}{(x_2 - 1)^2 + y_2^2} \quad (11)$$

$$y_3 = \frac{y_1 (x_2 - 1) - x_1 y_2}{(x_2 - 1)^2 + y_2^2} \quad (12)$$

2. CALCULATION OF THE CRYSTAL PARAMETERS

After subtracting the influence of Ccc, the complex impedance R_X now is to be transformed into the equivalent electrical diagram of the quartz crystal unit consisting of R_1, C_1, L_1 and C_0 , forming the crystal impedance Z according to fig. 6,

$$Z = (R_1 + j(\omega L_1 - 1/\omega C_1)) // j\omega C_0 \quad (13)$$

Basically, the four parameters can be derived from two measurements at different frequencies each yielding an impedance

$$R_X = \text{Re}(R_X) + j \text{Im}(R_X)$$

By means of the four values

- $\text{Re}(R_X(\omega_1))$
- $\text{Im}(R_X(\omega_1))$
- $\text{Re}(R_X(\omega_2))$
- $\text{Im}(R_X(\omega_2))$

the four crystal parameters can be calculated.

The two measuring frequencies must be located in the vicinity of the considered resonance, preferably on the right half of the admittance circle (see fig. 4). The spurious resonances of the crystal shall be well-isolated.

Experimental proofs have shown that the determination of C_0 from these measurements at frequencies close to the resonance lead to rather high errors for C_0 . A more precise measurement of C_0 can be performed at a frequency which is sufficiently apart from the considered crystal resonance. There, the motional branch of the crystal has a very high impedance and can be neglected. Thus, the measurement can be reduced to a pure capacitance measurement. From the measured voltages, the static capacitance C_0 could be calculated by the following formula:

$$-j 1/\omega C_0 = R_N \frac{(\underline{U}_k / \underline{U}_{rx} - 1)}{(\underline{U}_k / \underline{U}_{rn} - 1)} = j \text{Im}(R_X) \quad (14)$$

Ideally, the real part of the a. m. equation should be zero, however, an additional parallel loss resistance can be observed either due to measurement inaccuracy, i. e. in the vicinity of 90° -phase angle or because G_0 (fig. 3 c) cannot be neglected. Considering this, C'_0 has to be computed from:

$$C'_0 = - \text{Im}(R_X) / (\text{Re}(R_X)^2 + \text{Im}(R_X)^2) / \omega \quad (15)$$

ω - measuring frequency for C'_0 .

The above calculated capacitance also includes the cross-talk capacitance Ccc of the test jig. This capacitance has to be determined with an additional measurement with the Pi-network open circuited with the formula as in (14). The crystal C_0 is the difference $C'_0 - C_{cc}$.

With known C_0 , now the remaining circuit can be computed. The admittance of the complete crystal at the two measuring frequencies ω_1 and ω_2 is:

$$Y(\omega_1) = 1 / \{ \text{Re}(Z(\omega_1)) + j \text{Im}(Z(\omega_1)) \} = a_1 + j b_1 \quad (16)$$

$$Y(\omega_2) = 1 / \{ \text{Re}(Z(\omega_2)) + j \text{Im}(Z(\omega_2)) \} = a_2 + j b_2 \quad (17)$$

with

$$a_1 = \frac{\omega_1^2 R_1 C_1^2}{(1 - \omega_1^2 L_1 C_1)^2 + \omega_1^2 R_1^2 C_1^2} \quad (18)$$

$$b_1 = \frac{\omega_1 (C_1 + C_0) - \omega_1^3 (2 L_1 R_1 C_1 + L_1 C_1^2 - R_1^2 C_1^2 C_0) + \omega_1^5 L_1^2 C_1^2 C_0}{(1 - \omega_1^2 L_1 C_1)^2 + \omega_1^2 R_1^2 C_1^2} \quad (19)$$

$$a_2 = \frac{\omega_2^2 R_1 C_1^2}{(1 - \omega_2^2 L_1 C_1)^2 + \omega_2^2 R_1^2 C_1^2} \quad (20)$$

$$b_2 = \frac{\omega_2 (C_1 + C_0) - \omega_2^3 (2 L_1 R_1 C_1 + L_1 C_1^2 - R_1^2 C_1^2 C_0) + \omega_2^5 L_1^2 C_1^2 C_0}{(1 - \omega_2^2 L_1 C_1)^2 + \omega_2^2 R_1^2 C_1^2} \quad (21)$$

The four equations (18) to (21) contain three unknowns L1, C1 and R1, the fourth parameter, Co, has already been determined above. Solving these equations for L1, C1 and R1 leads to

$$L_1 = \frac{\omega_1 b_1^* - \omega_2 b_2^*}{\omega_1^2 - \omega_2^2} \quad (22)$$

$$C_1 = \frac{\omega_1^2 - \omega_2^2}{\omega_1^2 \omega_2 b_2^* - \omega_2^2 \omega_1 b_1^*} \quad (23)$$

$$R_1 = \frac{(a_1^* + a_2^*)}{2} \quad (24)$$

whereby

$$a^* + j b^* = \frac{1}{a + j(b - \omega C_0)} \quad (25)$$

R1 is computed from the arithmetic mean between both measurements.

3. ACCURACY OF THE MEASUREMENT

The accuracy depends on the following factors:

- arrangement of the Pi-network
- accuracy of the voltage and phase measurements
- accuracy of the calibration resistor
- accuracy of the Co-measurement

3.1 Measurement Errors Caused by the Arrangement of the Pi-Network

The mechanical arrangement has only very small influence on the accuracy. Theoretically, all error parameters are eliminated by the extended calibration. This is true, as long as the reflexions between power divider and Pi-network can be neglected.

Figure 7 shows the input reflexion coefficient of the Pi-network as a function of the resistance inserted in the Pi-network. This reflexion only plays a role if an imperfect power divider is used. This error could be suppressed by inserting an additional attenuation pad at the input of the Pi-network or by using a high performance (resistive) power divider connected with short leads.

Other possible errors can be caused by irradiation of RF-signals. They can be minimized by a compact and shielded construction of the arrangement. The cables should be double-screened and should be as short as possible. For the determination of Co, frequencies with high electromagnetic field (e. g. 10 MHz standard frequency) should be avoided. This can be verified by a trial Co-measurement at different frequencies.

3.2 Accuracy of the Voltage and Phase Measurement

The relative error for the calculation of Rx is:

$$\frac{dR_x}{R_x} = \frac{dK_1}{K_1} - \frac{dK_2}{K_2} + \frac{dR_n}{R_n} \quad (26)$$

DK1 / K1 relative error for voltage measurement with short circuit and with unknown impedance Rx

DK2 / K2 relative error for voltage measurement for short circuit and calibration resistor Rn

dRn / Rn relative error of Rn

a) influence of dK1 / K1

$$\frac{dK_1}{K_1} = \left[\frac{dU_k}{U_k} - \frac{dU_q}{U_q} \right] \frac{\left[1 - \frac{U_q}{U_k} \cos(\rho_k - \rho_{rx}) \right] - j \left[\frac{U_q}{U_k} \sin(\rho_k - \rho_{rx}) \right]}{\left[1 - \frac{U_q}{U_k} \cos(\rho_k - \rho_{rx}) \right]^2 + \left[\frac{U_q}{U_k} \sin(\rho_k - \rho_{rx}) \right]^2} \quad (27)$$

This equation describes the influence of the relative error for an erroneous measurement of the amplitude with

dUK/Uk relative error for short circuit measurement

dUq/Uq relative error with the crystal inserted

The result of this formula depends on the relative error of the network analyzer and on the magnitude of the impedance to be measured.

b) Influence of dK2 / K2

$$\frac{dK_2}{K_2} = \left[\frac{dU_k}{U_k} - \frac{dU_{rn}}{U_{rn}} \right] \frac{\left[1 - \frac{U_{rn}}{U_k} \cos(\rho_k - \rho_{rn}) \right] - j \left[\frac{U_{rn}}{U_k} \sin(\rho_k - \rho_{rn}) \right]}{\left[1 - \frac{U_{rn}}{U_k} \cos(\rho_k - \rho_{rn}) \right]^2 + \left[\frac{U_{rn}}{U_k} \sin(\rho_k - \rho_{rn}) \right]^2} \quad (28)$$

dUrn/Urn error of the voltage measurement with the calibration resistor inserted

For high measurement accuracy, the calibration resistor should have about the same magnitude as the resistance of the crystal, because then the influence of dK1/K1 equals that of dK2/K2 and the total error vanishes, which is not completely possible, as the crystal has a frequency dependent impedance. However, the residual error can be minimized by averaging of the measurement results at different frequencies or by iteratively stepping through different frequencies until a given repeatability is reached.

It was experimentally shown that with a high performance calibration resistor as described below, its value could be varied between 15 ohms and 100 ohms, and the mean values of the results are still within the accuracy limits of the method.

The figures 8 to 11 show the expected error for a 366 MHz /11th overtone crystal with the following parameters:

$f_s = 366,0911494$ MHz
 $L_1 = 2,25$ mH
 $C_1 = 0,084$ fF
 $R_1 = 220$ ohms
 $C_0 = 3,8$ pF

In figure 8, the maximum error of R_1 for an assumed amplitude error of $\pm 0,5\%$ is depicted. Different calibration resistors (25 ohms, 50 ohms and 100 ohms) are considered. In this example, both measurement frequencies are assumed to be located symmetrically with respect to f_s . The abscissa shows the magnitude of the difference of both measuring frequencies with respect to f_s . The best accuracy is achieved for $f = f_s$ with a maximum error of $\pm 1\%$. Using a 25 ohms calibration resistor and measuring frequencies located about ± 10 ppm around f_s , an error of less than $\pm 2\%$ can be expected. A frequency difference of 10 ppm is equivalent to an angle of

$$\beta = \arctan\left\{\left(\omega L_1 - 1 / \omega C_1\right) / R_1\right\} \approx 20^\circ \quad (29)$$

in the admittance circle (angle β is measured from the outer left point of the circle - see fig. 4).

Figure 9 shows the error for C_1 or L_1 , resp. Opposite to the results for R_1 , these parameters are best determined in a certain frequency offset of f_s of about $\pm 15 \dots \pm 25$ ppm equivalent to a phase angle β of $\pm 35 \dots \pm 50^\circ$. Then the minimum error is about $\pm 2\%$. If the frequency difference of the both measurement frequencies is too small, the relative error increases, because for small differences even rather small relative measurement errors may cause large absolute errors.

In figures 10 and 11 the error of R_1 , C_1 and L_1 , resp. is depicted for an expected phase measurement error of $\pm 0,1^\circ$. The parameter error is rather insensitive to the choice of the calibration resistor. In the average, the assumed phase error leads to an additional error of about $\pm 2\%$ for the determination of the crystal parameters.

3.3 Error of the Calibration Resistor

The error of the calibration resistor influences the computation of the impedance R_x directly. Therefore, it is strongly recommended to use very high precision resistors which are perfectly matched to the test jig for the application in the considered frequency range. We are using a thin-film resistor on a ceramic substrate. On its resistive film, the contracting pads are directly evaporated as gold layers with dimensions exactly fitting to the contact plane of the pi-network (see Fig. 12 a). The frequency response was tested

up to 1 GHz using the same technique as described above for quartz units. It was found that its electrical diagram as given in Fig. 12 can be simplified to a parallel connection of a pure resistor with a capacitor. Fig. 12 c shows the measured frequency response for this mode assuming different values for the parallel capacitance.

3.4 Error of C_0

The static capacitance C_0 is determined by an additional measurement considerably apart from the series resonance frequency f_s . The accuracy of the C_0 measurement is approximately $\pm 1\%$, if a number of measurements is averaged. The optimum location should be according to a recent agreement of IEC TC 49/Working group 6 as follows:

- For crystals up to 30 MHz, the measurement is made at 5 frequencies slightly above 30 MHz, i. e. 30.1, 30.2, 30.3, 30.4 and 30.5 MHz, and the average of the three values nearest the mean is used as the best estimate.

- For crystals above 30 MHz, measurements are recommended of three paired frequencies, each equidistant from f_s , i. e. $f_s (1 \pm .05)$, $f_s (1 \pm .06)$ and $f_s (1 \pm .02)$. For each pair, the value of C_0 is calculated of the lower and higher frequency, and a value of $C_0(i)$ obtained as the mean of the two C_0 values. This gives three estimates, $C_0, i = 1, 2, 3$. The best value to be used for C_0 is average of the two values which are closest to each other.

In either case, care should be given that the measurement frequencies are not coincidental with an unwanted mode of vibration.

4. MEASURING SEQUENCE

The measurement should be made under computer control. Based on the above described consideration of the achievable accuracy and the analysis of the error sources, the measurement sequence was optimized.

First, the calibration is performed by inserting consecutively a short-circuit, an open and a calibration resistor into the Pi-network and measuring the amplitude and phase at nominal frequency.

Then, the static capacitance C_0 is determined as described above.

From the nominal frequency given in the data sheet and from the expected Q-factor, two frequencies f_1 and f_2 are calculated, which are expected to be approximately $\pm 45^\circ$ off the nominal frequency with respect to the outer left point of the admittance circle. At these two frequencies, amplitude and phase are measured, and from this, first guess values for L_1', C_1' and R_1' are calculated.

From these, a first guess of the series resonance frequency f_s' can be computed by the Thompson formula.

The accuracy for the estimated parameters L1, C1, R1 depends very strongly on the location of the two frequencies which may be far from optimum at the first step. However, it was found that the frequency f_s derived from these L1 and C1 is already within about ± 1 ppm from the exact value, even for rather odd locations of f_1 and f_2 . From these data, two new frequencies can be computed, which lie more accurately within a phase offset of $\pm 40^\circ$ from f_s (with respect to the outer left point of the admittance circle). They are located rather symmetrically around f_s .

Now, a new measurement is performed at the two new frequencies and the motional parameters are calculated again, from which a new resonance frequency f_s can be computed. Its value is now compared with the frequency f_s' from the first guess. The frequency difference gives information about the achieved accuracy. Now, this procedure can be repeated until the difference of consecutive measurements for f_s and the motional parameters is within given tolerance limits. The final measurement is done at this series resonance frequency in order to determine the resistance R1 with a minimum error. From our experience, the frequency can thus be determined within $\pm 0,5$ ppm at 200 MHz and ± 1 ppm at about 500 MHz. The repeatability within one series of measurements is much better than this.

Finally, all computed data can be printed out.

5. COMPARATIVE MEASUREMENTS

In the graphs of fig. 13, some measurement results of different crystals are shown, which were achieved at 80 MHz, 200 MHz and 314 MHz on an international measurement workshop of Working Group 6 of the IEC Technical Committee TC 49, held in Bled/Yugoslavia in November 1988.

It can be seen that the results of this method are comparable in accuracy and reproducibility to those achieved with the S-parameter method of EIA 512. It could be shown that, due to the error correction, highly reproducible results can be achieved also with different constructions of the Pi-network.

REFERENCES:

- (1) Neuscheler, F: "Schwingquarz-Daten - mit Netzwerk-Analysatoren gemessen",
Elektronik 19 (18.09.1987)
155 - 162
- (2) Neubig, B. W. and Zimmermann, R.:

Recent Advances on the Measurement of Quartz Crystal Units up to 500 MHz and Above by the Use of a Pi-Network with Error Correction;
Proceedings of the 2nd International Conference on Frequency Control and Synthesis;
Leicester/UK (April 1989).

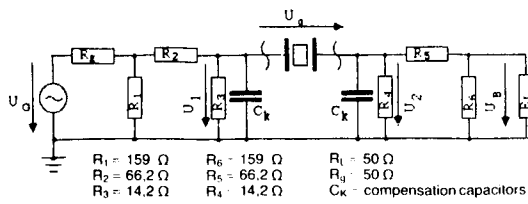
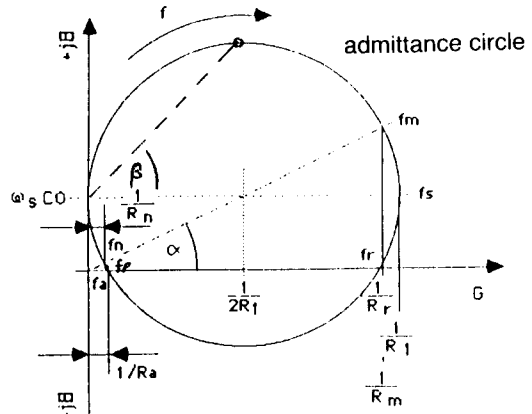


Fig. 1: Pi-network (IEC 444)



- fm: Maximum admittance- (minimum impedance-) frequency
- fs: Series resonance frequency
- fr: Resonance frequency with phase 0
- fa: anti resonance frequency (phase 0)
- fp: Parallel resonance frequency (loss-less)
- fn: Minimum admittance- (maximum impedance-) frequency
- Rr: resonance resistance
- R1: Series resonance resistance
- Rm: resistance at fm
- Ra: anti-resonance resistance

Fig. 4: Admittance circle of a quartz-crystal unit

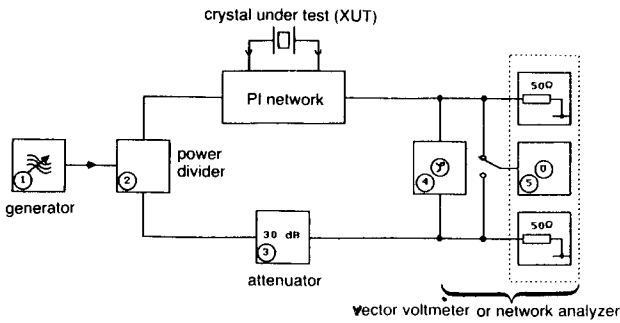
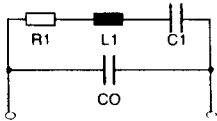
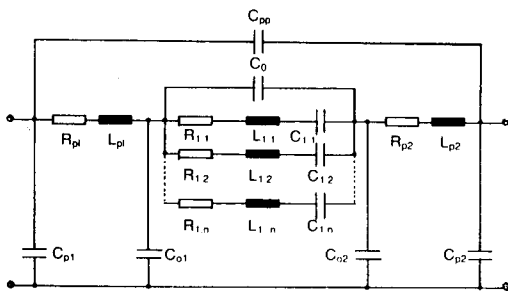


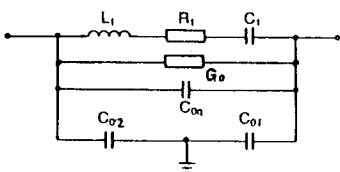
Fig. 2: Measurement set-up



3 a) Van Dyke diagram



3 b) extended version



3 c) proposed diagram

Fig. 3: equivalent electrical diagram of a quartz crystal unit Fig. 6: transformation

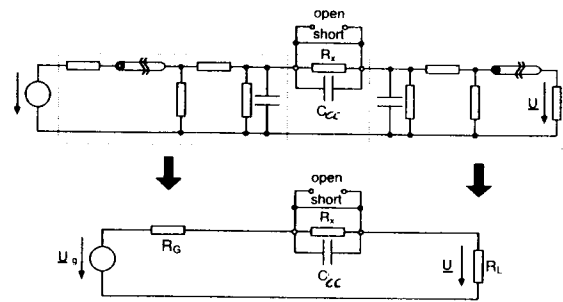
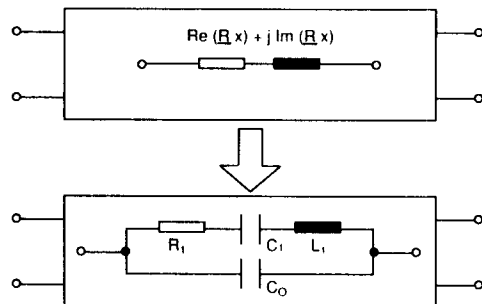


Fig. 5: calibration and measurement



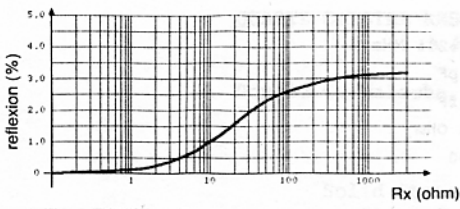


Fig. 7: Input reflexion coefficient of Pi-network

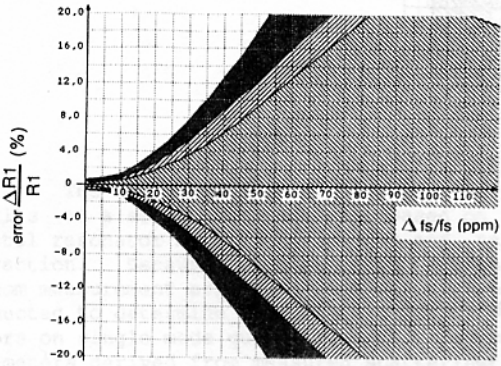


Fig. 8: R1-error due to amplitude error

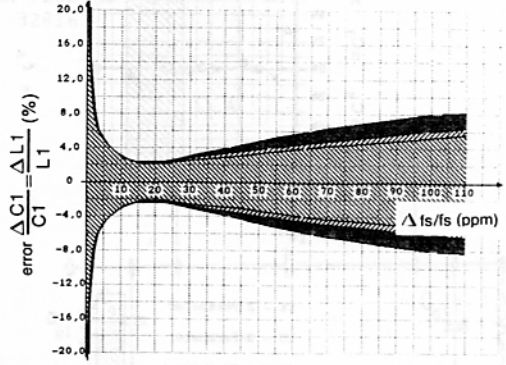


Fig. 9: C1, L1-error due to amplitude error of +/- 0,5 %

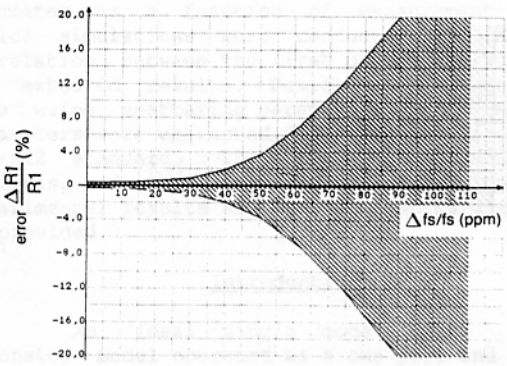


Fig. 10: R1-error due to phase error of +/- 0,1°

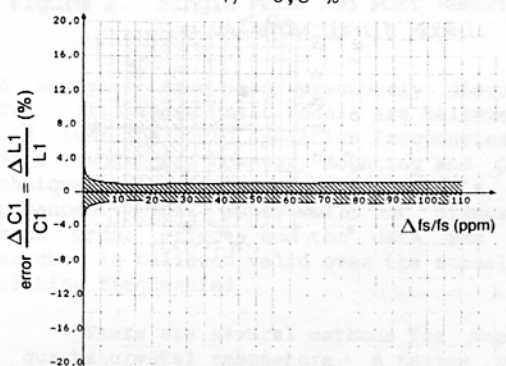
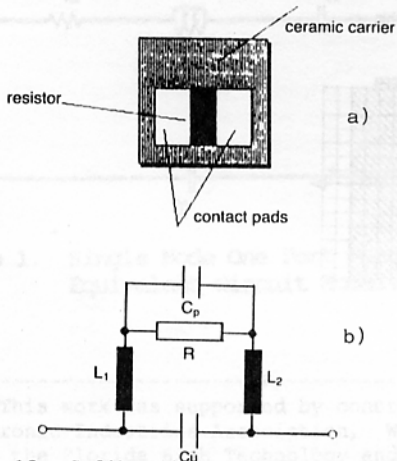


Fig. 11: C1-error due to phase error of +/- 0,1°



susceptance of calibration resistor

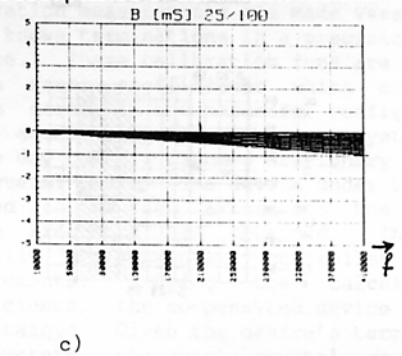


Fig. 12: Calibration resistor, its electrical diagram and frequency response

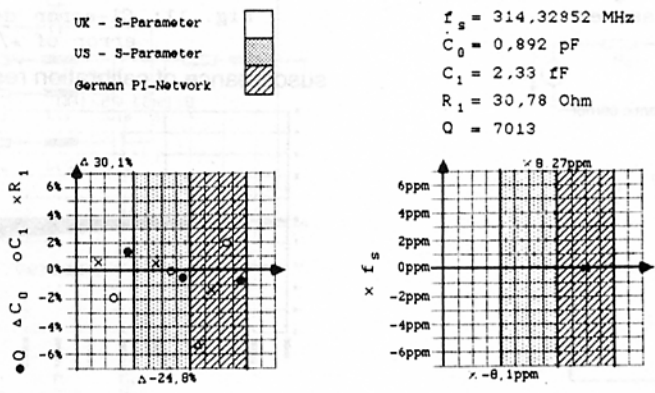
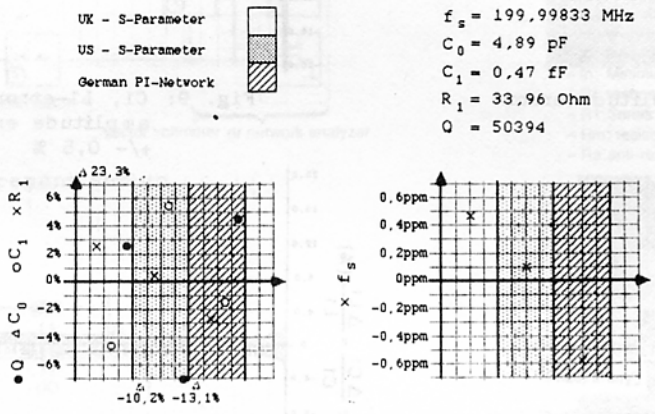
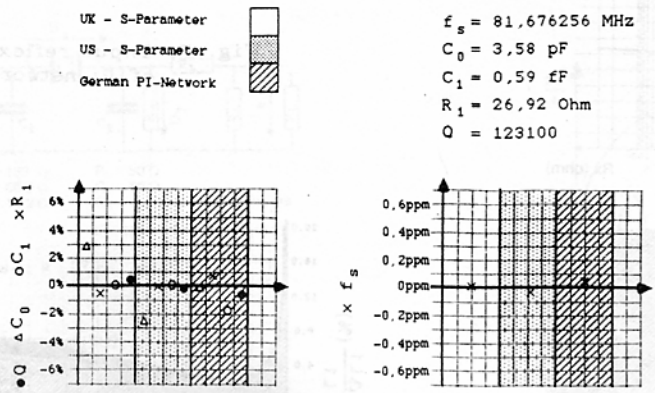


Fig. 13: Some results of comparative measurements
 Pi-network vs. S-parameter techniques
 (Bled, October 1988)